を用いて分散させる。それは、ナノ化処置またはナノカプセル化によって均一に分散（ELC 2009; Chaudhry, Watkins *et al.* 2010）させる。炭水化物（例えばデンプン）、ゼラチン、β-シクロデキストリンおよびアルギン酸カルシウムは、ナノキャリアの典型な例であり、数多くの企業が製造し、製品を販売（Möller, Eberle *et al.* 2009）している。乳化された非水溶性化合物は、もしかするとナノ範囲にある。しかしながら、キャリア（搬送）システムの場合は、サイズが大きくてもよい（Möller, Eberle *et al.* 2009）。

食品包装用ナノマテリアルおよびナノテクノロジーの応用は、食品接触材料や食品非接触材料の両方に該当し、急速に商用化になりつつある（Chaudhry and Castle 2011）。二酸化チタンおよびクレイ粒子のような単純な無機分子がパッケージに使用されているのに対し、食品中のカーボンナノチューブのような複雑な無機ナノ粒子の直接的な使用は、現在はないようである（Nanotechnology 2008）。食品接触材料の機能は、顔料、包装機能の改善、活性包装材料とインテリジェント食品包装、抗菌作用および台所用品の自己洗浄のカテゴリーに分類することができる。

顔料：食品接触材料のカーボンブラックおよび二酸化チタンを含む有機および無機顔料は、一般的に食品包装材料のプラスチック、板紙、缶の接着および密閉剤の発色剤として使用されている（Environment Canada 2011）。

包装器材の改善： 複合ナノマテリアルは、プラスチック母体にナノ物質を低レベル（2～5%）含有し、従来の食品包装材料に勝る幾つかの利点を示す。例えば、その利点は、機械的特性の改善、気体と液体の浸透性の減少および軽量化と難燃性の向上などである。複合ナノマテリアルは、主に瓶やフィルムの特性を改善し、場合によっては、他の材料のコーティングに用いられる。

特に、種々の有機クレイは、グローバルナノ対応の食品および飲料市場の約 70%に興味が持たれている（Möller, Eberle et al. 2009）。多くの複合材料は、成功裏にアジアおよび米国で商品化されている。例えばポリエチレン製（PET）ボトルの飲料（ジュース、ビールおよびソフトドリンク）の炭酸ガスの低減と酸素の侵入を最小限にする（Nanotechnology 2008; Duncan 2011）。クレイの低コスト化のために肉、チーズおよび穀物などの製品用の様々な食品包装用途用ナノクレイポリマー複合材料が開発された。これらナノクレイポリマー複合材料は、フルーツジュースおよび乳製品用の包装の押出コーティング用すなわち、炭酸飲料のボトル製造の共押し出し法に使用される（Hatzigrigoriou and Papaspyrides 2011）。

異なるナノマテリアルは、食品包装の改善ために、すなわちバリア性または機能的特性を向上のために、純粋なポリマーまたは複合ナノマテリアルに添加することができる。例えば、材料の剛性および強度の改善のために窒化チタンがある（Chaudhry and Castle 2011）。二酸化チタンナノ粒子は、材料の透明性を維持しながら UV 光をブロックするためにフィルムに添加することができ（Chaudhry and Castle 2011）また、アクリルナノ粒子は、ポリ乳酸フィルムを強化するために添加することができると述べている（Robinson and Morrison 2010）。また、この 2 つのナノマテリアルは、上述した品質改善の目的で市販されている。二酸化ケイ素は、ナノ粒子の真空蒸着法でフィルム上に蒸着させ、炭酸飲料やスナック、菓子およびコーヒーの貯蔵期間を延長させるために使用される（Silvestre, Duraccio et al. 2011）。

活性包装材料とインテリジェント食品包装：活性物質および材料は、貯蔵期間の延長の維持または包装食品の状態を劣化させない目的で添加される。その作用は、包装食品または食品を取り巻く環境からの物質の吸収または放出させるためである。具体的には、欧州市場における活性包装の現状を以下に述べる。活性包装システムによる製品は、食べることが出来ないことを消費者に対して明確に識別出来るように表示・啓蒙しなくてはならない。そして新しい活性または高機能物質は、EFSA によって承認されなければならない。酸化亜鉛、銀、リン酸カルシウムまたは銀ゼオライトのナノ粒子を含むポリマー複合材料に抗菌剤を加えた商品は、販売されている（Robinson and Morrison 2009）。

金および二酸化チタンのナノ粒子から製造されたナノセンサーは、食品包装ラインで食品の状態の監視システムに利用できる。ヨーロッパの幾つかの開発初期段階のナノセンサーは、製品が受け入れられる可能性が高いか否かを検索するため市販されている（Robinson and Morrison 2010）。

抗菌作用および自浄作用を持つ台所用品：幾つかの企業は、冷蔵庫、冷凍庫およびコーヒ

ーマシンを製造している。これらの製品は、ナノサイズの銀および二酸化チタンを含み微生物の増殖を防止し、製品の衛生的な環境を維持するために、内面および表面にナノマテリアルが添加されている。同様に、ナノサイズの銀でコーティングされた抗菌台所用品（例えば刃物類、平鍋、まな板、食品容器　およびサラダボウル）は、実用化されている（Miller, Lowrey et al. 2008）。これらの製品は、デンマークの市場で確認されていない。しかし、これら製品は、容易にオンラインで購入することができる。

過去10年、多くのメーカーは、ナノサイズ銀を使用し、抗菌作用を持つ冷蔵庫、冷凍庫および洗濯機を販売してきたが、これらの製品の大半は、もはや市場から撤退した。2005年に一つの大きな台所家電のメーカーは、抗菌製品の製品ラインを立ち上げたが、NGOの国民の反発と圧力によって一時的に市場から撤退した（El-Badawy, Feldhake et al. 2010）。

D．考察

欧州では、2011年にナノマテリアルの定義が確定してから、各国でナノマテリアルに対する（義務的な）登録制度が普及しつつあり、2012年最初に導入したフランスをはじめとして、デンマーク、ベルギーでも登録制度が開始された。しかし、この登録制度は、化学物質の登録システムである REACH の対象物質に限定されており、食品及び飼料、食品接触材、医療器具、化粧品、農薬、及び廃棄物などは適用除外となっている。一方、新規食品および新規食品組成、規制（EC）258/97）においては、ナノマテリアルに限らず、新規の物質を含む食品は規制の対象となり、特に食品添加物のナノ形態で開発されていた場合、それは新たな添加剤と考えられ、事前に販売承認を必要となる。しかし、1997年以前から使われているナノマテリアルを含む可能性のある物質を含む食品は対象外であり、安全性や曝露に関する情報は不明なままである。この状況に関しては、既存物質を対象にEFSAが評価を行っている。食品包装中のナノマテリアルに関しても既存物質のいくつかはEFSAにより評価されている。

以上のように、一般の化学物質に関しての登録制道は整いつつあるが、食品関連に関しての情報は、既存物質を除いて、まだ規制当局に情報が届けられていない状況である。このことは欧州における食品関連業界が新規のナノマテリアルを用いた商品化に慎重である状況を示し、さらに抗菌作用を謳ったナノ銀を含む家電製の回収もあったことからも社会的な需要に壁があるように思われる。しかし、研究レベルでは文献調査等の結果から、ヨーロッパと世界の食品および飼料メーカーにおける潜在的なナノマテリアル需要が存在することを示している。また、欧州では食品分野におけるナノテクノロジーの大型の開発研究プロジェクト（NanoPack, Good Food project (FP6), Natural Antimicrobials for Innovative Safe Packaging (FP7)等）も実施されており、将来的なニーズは決して低くはないと思われる。

食品及び飼料等に関する文献調査等では、重要な潜在的需要の可能性があるナノマテリアルとして、二酸化ケイ素/シリカ、二酸化チタン、顔料およびナノキャリアシステムが挙げられるが、これらはほとんど添加剤であり、典型的には、最終的な食品および飼料製品中に少量（食品では＜0.01～1%（w/w）および飼料では1～4%（w/w））が添加されるというものである。食品および飼料中のナノマテリアルの使用は、法律によって規制されているが、現時点ではEFSA等で行っている既存のナノマテリアルの評価の動向を注視している状況であるとも考えられ、評価の方向性が定まれば、新規製品の申請へと急速に動き出すかも知れない。

食品包装関連では、二酸化ケイ素、窒化チタンおよびカーボンブラックは、現在の欧州法により食品包装用に認可されている3つのナノマテリアルであるが、その他の多くの可能な材料は、世界の市場で研究開発されている。有機・無機の顔料は、今のところ適用除外品である。文献調査による潜在的可能性の製品タイプとしては、プラスチックフィルムとプラスチック容器があり、重要な潜在的可能性のナノマテリアルとしてはカーボンブラック、二酸化ケイ素、窒化チタン、複合ナノマテリアル（ナノクレイ、金属および金属酸化物ナノ粒子；2～5%含有（w/w））が示された。それらの使用目的としては、顔料に加え、従来の食品包装容器の機械的向上やバリア特性の改善、抗菌性や食品のモニタリング等が挙げられており、現在は、ナノマテリアルの食品包装への適用は登録が必要ではあるが、使用が許可された場合には、その使用はゆっくりと増加していくと予想される。

E．結論

ナノマテリアルの食品関連分野を中心とした

曝露状況に関する国際動向を調査すること目的として、26年度は、ナノマテリアルに関する規制が比較的進んでいる欧州における、食品分野への適用実態を検討した。まず、ナノ関連に関する欧州のの規制動向については、2011年にナノマテリアルの定義が確定して以降、各国でナノマテリアルに対する登録制度が普及しつつあるが、一般の化学物質の登録システムを中心としたもので、食品及び飼料、食品接触材、医療器具、化粧品、農薬、及び廃棄物などは適用除外となっている。一方、新規食品規制においては、ナノマテリアルに限らず、新規の物質を含む食品は規制の対象となるものの、既存のナノマテリアルを含む可能性のある物質を含む食品は対象外である。現時点では新規のナノマテリアルとしての登録は認められていない。しかし、研究開発に関する文献調査等の結果からは、ヨーロッパと世界の食品および飼料メーカーにおける潜在的なナノマテリアル需要が存在することが示された。食品及び飼料等に関する文献調査等では、重要な潜在的需要の可能性があるナノマテリアルとして、二酸化ケイ素/シリカ、二酸化チタン、顔料およびナノキャリアシステムが挙げられ、食品包装関係では、カーボンブラック、二酸化ケイ素、窒化チタン、複合ナノマテリアルなどがあげられる。これらの物質の評価手法がある程度定まれば、新規のナノマテリアルの適用も増加していくものと考えられた。

G. 研究発表

（論文発表）

Hashiguchi, S., Yoshida, H., Akashi, T., Komemoto, K., Ueda, T., Ikarashi, Y., Miyauchi, A., Konno, K., Yamanaka, S., Hirose, A., Kurokawa, M., Watanabe, W. Titanium dioxide nanoparticles exacerbate pneumonia in respiratory syncytial virus (RSV)-infected mice. Environ. Toxicol. Pharmacol. (2015) 39, 879-886.

Ohba T, Xu J, Alexander DB, Yamada A, Kanno J, Hirose A, Tsuda H, Imaizumi Y. MWCNT causes extensive damage to the ciliated epithelium of the trachea of rodents. J Toxicol Sci. 39:499-505. (2014)

Xu J, Alexander DB, Futakuchi M, Numano T, Fukamachi K, Suzui M, Omori T, Kanno J, Hirose A, Tsuda H. Size- and shape-dependent pleural translocation, deposition, fibrogenesis, and mesothelial proliferation by multiwalled carbon nanotubes. Cancer Sci. 105:763-9. (2014)

Cui H, Wu W, Okuhira K, Miyazawa K, Hattori T, Sai K, Naito M, Suzuki K, Nishimura T, Sakamoto Y, Ogata A, Maeno T, Inomata A, Nakae D, Hirose A, Nishimaki-Mogami T. High-temperature calcined fullerene nanowhiskers as well as long needle-like multi-wall carbon nanotubes have abilities to induce NLRP3-mediated IL-1beta secretion. *Biochem Biophy Res Commun,* 452 : 593-599. (2014)

（学会発表）

Norihiro Kobayashi, Reiji Kubota, Ryota Tanaka, Hiroshi Takehara, Masato Naya, Yoshiaki Ikarashi, Akihiko Hirose: Evaluation of teratogenicity of multi-wall carbon nanotubes in pregnant mice after repeated intratracheal instillation. 54th Annual Meeting of the Society of Toxicology (SOT 2015) (2015.3 San Diego, CA, USA).

Seiko Hashiguchi, Hiroki Yoshida, Toshi Akashi, Akihiko Hirose, Masahiko Kurokawa, Wataru Watanabe, Effects of titanium dioxide nanoparticles on the pneumonia in respiratory syncytial virus-infected mice. EUROTOX2014 (2014.9, Edinburgh)

菅野 純、高橋祐次、高木篤也、広瀬明彦、Toxicological considerations for particulate matter as foreignbody carcinogen. 第73回日本癌学会学術総会 (2014.9) 横浜、シンポジウ

菅野 純, 高橋 祐次、高木 篤也, 広瀬 明彦, 今井田 克己, 津田 洋幸、ナノマテリアルの吸入毒性評価の迅速化と効率化に向けて、第41回 日本毒性学会学術年会、2014年7月、神戸、シンポジウム

小林憲弘, 田中亮太, 竹原広, 納屋聖人, 久保田領志, 五十嵐良明, 広瀬明彦：マウス反復気管内投与による多層カーボンナノチューブの催奇形性の評価. 第41回日本毒性学会学術年会 (2014.7.2 兵庫県神戸市).

坂本義光，小縣昭夫，北条　幹，山本行男，広瀬明彦，井上義之，橋爪直樹，猪又明子，中江 大，“ラットにおいて多層カーボンナノチューブの経気管噴霧反復投与が及ぼす影響”第41回日本毒性学会学術年会　(2014年7月4日．兵庫県神戸市)

G．知的財産権の出願・登録状況（予定を含む）

1．特許取得
（該当なし）
2．実用新案登録
（該当なし）
3．その他
（該当なし）

研究成果の刊行に関する一覧表

書籍

著者氏名	論文タイトル名	書籍全体の編集者名	書　籍　名	出版社名	出版地	出版年	ページ
該当なし							

雑誌

発表者氏名	論文タイトル名	発表誌名	巻号	ページ	出版年
Hashiguchi S, Yoshida H, Akashi T, Komemoto K, Ueda T, Ikarashi Y, Miyauchi A, Konno K, Yamanaka S, Hirose A, Kurokawa M, Watanabe W.	Titanium dioxide nanoparticles exacerbate pneumonia in respiratory syncytial virus (RSV)-infected mice.	Environ. Toxicol. Pharmacol.	39	879-886	2015
Ohba T, Xu J, Alexander DB, Yamada A, Kanno J, Hirose A, Tsuda H, Imaizumi Y.	MWCNT causes extensive damage to the ciliated epithelium of the trachea of rodents.	J Toxicol Sci.	39	499-505	2014
Xu J, Alexander DB, Futakuchi M, Numano T, Fukamachi K, Suzui M, Omori T, Kanno J, Hirose A, Tsuda H.	Size- and shape-dependent pleural translocation, deposition, fibrogenesis, and mesothelial proliferation by multiwalled carbon nanotubes.	Cancer Sci.	105	763-769	2014
Cui H, Wu W, Okuhira K, Miyazawa K, Hattori T, Sai K, Naito M, Suzuki K, Nishimura T, Sakamoto Y, Ogata A, Maeno T, Inomata A, Nakae D, Hirose A, Nishimaki-Mogami T.	High-temperature calcined fullerene nanowhiskers as well as long needle-like multi-wall carbon nanotubes have abilities to induce NLRP3-mediated IL-1beta secretion.	Biochem Biophy Res Commun	452	593-599	2014

ENVIRONMENTAL TOXICOLOGY AND PHARMACOLOGY 39 (2015) 879–886

Available online at www.sciencedirect.com

ScienceDirect

journal homepage: www.elsevier.com/locate/etap

Titanium dioxide nanoparticles exacerbate pneumonia in respiratory syncytial virus (RSV)-infected mice

Seiko Hashiguchi[a], *Hiroki Yoshida*[b], *Toshi Akashi*[c], *Keiji Komemoto*[a], *Tomoyuki Ueda*[a], *Yoshiaki Ikarashi*[d], *Aki Miyauchi*[c], *Katsuhiko Konno*[b], *Sayoko Yamanaka*[b], *Akihiko Hirose*[e], *Masahiko Kurokawa*[b], *Wataru Watanabe*[a,*]

[a] *Department of Microbiology, Graduate School of Clinical Pharmacy, Kyushu University of Health and Welfare, 1714-1 Yoshino, Nobeoka, Miyazaki 882-8508, Japan*

[b] *Department of Biochemistry, Graduate School of Clinical Pharmacy, Kyushu University of Health and Welfare, 1714-1 Yoshino, Nobeoka, Miyazaki 882-8508, Japan*

[c] *Department of Microbiology and Infectious Diseases, School of Pharmaceutical Sciences, Kyushu University of Health and Welfare, 1714-1 Yoshino, Nobeoka, Miyazaki 882-8508, Japan*

[d] Division of Environmental Chemistry, National Institute of Health Sciences, 1-18-1 Kamiyoga, Setagaya-ku, Tokyo 158-8501, Japan

[e] *Division of Risk Assessment, Biological Safety Research Center, National Institute of Health Sciences, 1-18-1 Kamiyoga, Setagaya-ku, Tokyo 158-8501, Japan*

ARTICLE INFO

Article history:
Received 4 November 2014
Received in revised form
23 February 2015
Accepted 24 February 2015
Available online 3 March 2015

Keywords:
Titanium dioxide
Nanoparticles
Respiratory syncytial virus
Pneumonia

ABSTRACT

To reveal the effects of TiO_2 nanoparticles, used in cosmetics and building materials, on the immune response, a respiratory syncytial virus (RSV) infection mouse model was used. BALB/c mice were exposed once intranasally to TiO_2 at 0.5 mg/kg and infected intranasally with RSV five days later. The levels of IFN-γ and chemokine CCL5, representative markers of pneumonia, in the bronchoalveolar lavage fluids of RSV-infected mice had increased significantly in TiO_2-exposed mice compared with the control on day 5 post-infection, but not in uninfected mice. While pulmonary viral titers were not affected by TiO_2 exposure, an increase in the infiltration of lymphocytes into the alveolar septa in lung tissues was observed. Immunohistochemical analysis revealed aggregation of TiO_2 nanoparticles near inflammatory cells in the severely affected region. Thus, a single exposure to TiO_2 nanoparticles affected the immune system and exacerbated pneumonia in RSV-infected mice.

Abbreviations: TiO_2, titanium dioxide; RSV, respiratory syncytial virus; IFN-γ, interferon-gamma; BALF, bronchoalveolar lavage fluids; BFRs, brominated flame retardants; DBDE, decabrominated diphenyl ether; TBBPA, tetrabromobisphenol A; PBS, phosphate-buffered saline; IL, interleukin; PFU, plaque-forming units; ELISA, enzyme-linked immunosorbent assay; LPS, lipopolysaccharide.

* *Corresponding author.* Tel.: +81 982 23 5685; fax: +81 982 23 5685.
E-mail address: w_watal@phoenix.ac.jp (W. Watanabe).

http://dx.doi.org/10.1016/j.etap.2015.02.017
1382-6689/

1. Introduction

Nanomaterials are engineered structures with at least one dimension of 100 nm or less (Nel et al., 2006). Various kinds of nanomaterials are known and have a wide range of applications (Maidalawieh et al., 2014; Nel et al., 2006; Stamatoiu et al., 2012). Titanium dioxide (TiO_2) nanoparticles are used in cosmetics and building materials because they are chemically and thermally stable. When research focused on TiO_2 nanoparticles were in drug delivery systems (Zhang et al., 2012) several findings of toxicity due to exposure to TiO_2 nanoparticles were reported, such as carcinogenesis of the lung in rats (Xu et al., 2010), induction of strong oxidative stress and mitochondrial damage in glial cells (Huerta-Garcia et al., 2014), and inflammatory disorder on the cardiovascular system in ApoE knockout mice (Chen et al., 2013). Although we are exposed to TiO_2 nanoparticles in daily life, the safety of TiO_2 nanoparticles for human health is poorly known.

Human respiratory syncytial virus (RSV), a member of the *Paramyxoviridae* family, is a prevalent infectious agent of acute lower respiratory illness in infants and young children (MacDonald et al., 1982). An initial RSV infection is frequent during the first few years of life, and most children have been infected by 24 months of age (Collins et al., 2001). Clinically severe RSV infection is seen primarily in infants and young children with naïve immune systems and/or genetic predispositions (Holberg et al., 1991) and patients with suppressed T-cell immunity (MacDonald et al., 1982). RSV reinfects adults at a rate of approximately 5–10% per year (Falsey, 2007), and is an important cause of morbidity and mortality in the elderly (Falsey et al., 2005). Thus, because the severity of RSV infection reflects the condition of the host immunity, we established a novel assay system for evaluation of the immunotoxicity of the brominated flame retardants (BFRs) using a murine model of RSV infection (Watanabe et al., 2008a). We subsequently demonstrated that decabrominated diphenyl ether (DBDE) (Watanabe et al., 2008b, 2010a) and tetrabromobisphenol A (TBBPA) (Takeshita et al., 2013; Watanabe et al., 2010b) caused developmental immunotoxicity and irregular production of cytokines in RSV-infected mice, respectively. In addition, we also revealed that perinatal exposure to methamidophos, a representative organophosphate insecticide, suppressed the production of proinflammatory cytokines using this model (Watanabe et al., 2013).

In the present study, we adopted the RSV infection mouse model to evaluate the effects of TiO_2 nanoparticles on the immunotoxicity after a single exposure. Then we investigated the effects of TiO_2 nanoparticles on pneumonia in RSV infection by focusing on the variations in of cytokine and chemokine levels in bronchoalveolar lavage fluid (BALF) and the exacerbation of pneumonia in lung tissues by histopathological assay.

2. Materials and methods

2.1. Animals

Female (5 weeks old) BALB/c mice were purchased from Kyudo Animal Laboratory (Kumamoto, Japan) and housed at 25 ± 2 °C. The mice were allowed free access to the conventional solid diet CRF-1 (Oriental Yeast Co., Chiba, Japan) and water and used in this experiment after 7 d acclimation. The animal experimentation guideline of the Kyushu University of Health and Welfare were followed in the animal studies.

2.2. Cell and virus

The A2 strain of RSV was obtained from American Type Culture Collection (ATCC, Rockville, MD) and grown in HEp-2 cell (human epidermoid carcinoma, ATCC CCL-23) cultures. Viral titers of HEp-2 cells were measured by the plaque method (Watanabe et al., 2008a) and expressed as plaque-forming units per milliliter (PFU/mL).

2.3. Chemical compound

TiO_2 nanoparticles were kindly provided by Tayca Corp. (Osaka, Japan). The particles form ultra-fine rutile crystals primarily 35 nm in diameter. TiO_2 nanoparticles readily aggregate to form microparticles in phosphate-buffered saline (PBS). To avoid aggregation, the suspension of TiO_2 nanoparticles in PBS was dispersed using a portable ultrasonic disruptor just before treatment of mice. Then the mean secondary diameter of the particles was 913 nm, ranging from 804 to 1022 nm, as measured by a Zetasizer Nano (Malvern Instruments, Worcestershire, UK).

2.4. Animal tests

Six-week-old mice were intranasally administered 0.1 mL of a suspension of TiO_2 nanoparticles at 0.25 or 2.5 mg/kg of body weight one time under anesthesia for histological assays or 0.5 mg/kg for measuring cytokines in BALF and pulmonary viral titers. In control group, mice were given PBS intranasally under anesthesia.

The RSV infection test was performed as reported previously (Watanabe et al., 2008a). Briefly, 5 d after from TiO_2 exposure, mice were infected intranasally with 3.5×10^5 PFU of the A2 strain of RSV under anesthesia. In a mock-infected group, mice were given PBS intranasally. On day 5 after infection, blood samples were prepared from RSV-infected mice under anesthesia and BALF was obtained from the mice under anesthesia by instilling 0.8 mL of cold PBS into the lungs and aspirating it from the trachea using a tracheal cannula. Following the acquisition of BALF, the lungs were removed, immediately frozen in liquid N_2, and stored at −80 °C until virus titration. Ice-cold BALF was centrifuged at 160 × *g* at 4 °C for 10 min. After centrifugation, the supernatant was stored at −80 °C until to use. The cell pellet was suspended in 0.3 mL of cellbanker-1 (Nippon Zenyaku Kogyo Co., Ltd., Koriyama, Japan) as bronchoalveolar lavage cells, and then stored at −80 °C prior to use. Frozen lung tissue was homogenized with cold quartz sand in a homogenizer. After centrifugation at 480 × *g* at 4 °C for 15 min, the supernatants of the homogenates were used for a plaque assay. Viral titers in lungs of mice were expressed as PFU/mL.

2.5. ELISA

Interleukin (IL)-2, IL-4, IL-10, and interferon (IFN)-γ levels in BALF were measured using specific ELISA kits (Ready-set-go, eBioscience Inc., San Diego, CA) according to the manufacturer's instructions. Levels of CCL5 (RANTES) in BALF and serum and CCL3 (MIP-1α) in BALF and the culture supernatant of bronchoalveolar lavage cells were measured using specific ELISA kits (Quantikine, R&D Systems, Inc., Minneapolis, MN) according to the manufacturer's instructions. The lower limits of detection of the kits are 2 (pg/mL) for IL-2, 4 (pg/mL) for IL-4, 8 (pg/mL) for IL-10, 15 (pg/mL) for IFN-γ, 2 (pg/mL) for CCL5, and 1.5 (pg/mL) for CCL3. The intra- and interassay coefficients of variation for the ELISA results were less than 10%.

2.6. Flow cytometric analysis of bronchoalveolar lavage cells

Flow cytometric analysis was performed according to our previous report (Takeda et al., 2014). Briefly, bronchoalveolar lavage cells were stimulated with BD GolgiStop (BD PharMingen, San Diego, CA) at 1 μL/mL for 6 h at 37 °C. After incubation, the cells were washed twice and stained for intracellular IFN-γ (FITS Rat Anti-Mouse IFN-γ, BD PharMingen, San Diego) and IL-4 (PE Rat Anti-Mouse IFN-γ, BD PharMingen, San Diego), according to the manufacturer's instructions. The cells were washed twice and analyzed on an FACS Calibur 35 flow cytometer (Becton Dicknson, Sunnyvale, CA).

2.7. Histological methods and evaluation

For histological examination of RSV-infected lungs, 3–5 mice per group of infected mice were sacrificed by cervical dislocation on day 5 after infection, and the lungs were removed and placed in buffered formalin for a minimum of 24 h. The tissue was then embedded in low-melting point paraffin, sectioned at a thickness of 5 μm, and stained with hematoxylin and eosin. After taking two pictures randomly of each pulmonary lobe using a microscope (×100), the pictures were analyzed for the proportion of alveolar septa and infiltration of the inflammatory cells into the tissues per unit area by Adobe Photoshop (Adobe Systems, Inc., San Jose, CA).

2.8. Immunohistochemical evaluation

The lung tissue sections were deparaffinized and hydrated through xylenes and graded alcohols. After washing with water, they were incubated in unmasking solution (Vector Laboratories, Inc., Burlingame, CA) at 90 °C for 30 min. Then, the sections were incubated in the 0.3% H_2O_2 in PBS for 30 min to quench the endogenous peroxidase activity and treated with blocking serum (Vector Laboratories, Inc.) for 30 min. The lung tissues were stained with a goat polyclonal antibody against RSV protein (1:250, Acris Antibodies GmbH, Inc., San Diego, CA) for 90 min. Then, RSV proteins were detected using a VECTASTAIN ABC kit (Vector Laboratories, Inc.) according to the manufacturer's instructions. The sections were faintly counterstained with hematoxylin.

2.9. Culture of bronchoalveolar lavage cells

Culture of bronchoalveolar lavage cells obtained from RSV-infected mice on day 1 post-infection was performed according to our previous report (Watanabe et al., 2010a). Briefly, 200 μL of bronchoalveolar lavage cells suspension (2.5×10^5 cells/mL) was seeded on each well in a 96-well microtiter plate and incubated at 37 °C for 24 h in a humidified air with 5% CO_2. After incubation, the culture medium was removed by aspiration and replaced in fresh RPMI medium with or without 0.1 mg/mL of TiO_2 nanoparticles. Following 24 h further incubation, the culture medium was removed by aspiration and replaced in fresh RPMI medium with or without 100 ng/mL of lipopolysaccharide (W E. coli 0127: B8, Difco, Detroit, MI; LPS) for 24 h. The culture supernatant was harvested from each well and the amount of CCL3 was measured by ELISA.

2.10. Statistical analysis

Comparisons between the pulmonary viral titers and the levels of cytokines and chemokines of the control and TiO_2-treated groups were carried out using Student's *t*-test. A *P* value of 0.05 or less was considered to be significant.

3. Results

3.1. Effects of TiO_2 nanoparticles on RSV infection in mice

To investigate the effects of TiO_2 nanoparticles on the immune response to RSV infection, six-week-old female BALB/c mice were exposed intranasally to 0.1 mL of TiO_2 suspension at 0.5 mg/kg of body weight under anesthesia. No abnormal behavior or dystrophy due to the stress of TiO_2 exposure was observed compared to the control (0 mg/kg) in the mice, and the mice were infected intranasally with the A2 strain of RSV at 3.5×10^5 PFU five days after TiO_2 exposure. The levels of IFN-γ, a representative marker of pneumonia in RSV infection, in BALF were measured on day 5 post-infection (Table 1). The IFN-γ levels of RSV-infected mice treated with TiO_2 were significantly ($P < 0.05$) higher than those in the control. In mock-infected mice treated with or without TiO_2, the levels of IFN-γ in BALF were under the limit of detection. These results indicated that pneumonia in RSV-infected mice was exacerbated by TiO_2 exposure. To investigate further effects of exposure to TiO_2 on the immune system of RSV-infected mice, the levels of Th1 cytokines (IFN-γ and IL-2) and Th2 cytokines (IL-4 and IL-10) in BALF were also measured on day 5 after infection (Table 1). The levels of IL-10 in BALF were significantly ($P < 0.05$) increased by approximately 92% compared with the control. No significant increase of IL-2 in BALF was found after TiO_2 treatment, and the levels of IL-4 in BALF were under the limit of detection. In mock-infected mice treated with or without TiO_2, the levels of cytokines in BALF were under the limit of detection. To reveal effects of exposure to TiO_2 on the Th1/2 immune balance of RSV-infected mice on day 5 post-infection, intracellular IFN-γ and IL-4 productions by the bronchoalveolar lavage cells were examined by flow cytometry (Table 2).

Table 1 – Effects of TiO_2 on levels of cytokines in BALF of RSV-infected mice on day 5 post-infection.

TiO_2 exposure (mg/kg)	Concentration (ng/mL)[a]							
	RSV-infected				Mock-infected			
	IFN-γ	IL-2	IL-4	IL-10	IFN-γ	IL-2	IL-4	IL-10
0	8.59 ± 3.44	0.02 ± 0.01	<0.01	1.65 ± 0.71	<0.01	<0.01	<0.01	<0.01
0.5	12.90 ± 2.10*	0.03 ± 0.01	<0.01	3.17 ± 1.15*	<0.01	<0.01	<0.01	<0.01

[a] Concentration (ng/mL) of each cytokine in BALF from RSV-infected mice treated with or without TiO_2 (0.5 mg/kg) was measured by ELISA for each specific cytokine. Data represents mean values of 3–6 mice. Numbers in parentheses indicate standard deviation.
* Statistically different from control at $P < 0.05$ (Student's t-test).

Table 2 – Effects of TiO_2 on intracellular cytokine levels in bronchoalveolar lavage cells on day 5 post-infection from RSV-infected mice.

TiO_2 exposure (mg/kg)	% of total population[a]			
	IFN-γ⁻IL-4⁻	IFN-γ⁺IL-4⁻	IFN-γ⁻IL-4⁺	IFN-γ⁺IL-4⁺
0	98.7	1.1	0.1	0.1
0.5	98.9	0.8	0.1	0.2

[a] Bronchoalveolar lavage cells were collected from RSV-infected mice treated with or without TiO_2 (0.5 mg/kg) on day 5 post-infection. The pooled bronchoalveolar lavage cells were stimulated BD GolgiStop for 6 h at 37 °C and stained intracellular IFN-γ and IL-4. The stained cells were analyzed by flow cytometry.

There was not a significant change in the population of IFN-γ-positive cells and IL-4-positive cells due to TiO_2 treatment. These results suggested that TiO_2 exposure should affect the immune response to RSV infection.

Chemokine CCL5 is a common marker of the severity of inflammation in the lungs due to RSV infection (Lambert et al., 2003) and chemokine CCL3 also is an inflammatory marker. Therefore, we measured the levels of CCL5 and CCL3 in BALF on day 5 after infection (Table 3). The levels of CCL5 in BALF were significantly ($P < 0.05$) increased by approximately 36% compared with the control, but there was no significant increase of CCL3 levels in TiO_2-exposed mice. In mock-infected mice treated with or without TiO_2, the levels of chemokines in BALF were under the limit of detection. The levels of CCL5 in serum were significantly ($P < 0.05$) increased by approximately 31% compared with the control (Table 3). Thus, these results strongly suggested that TiO_2 exposure exacerbated the pneumonia due to RSV infection.

To evaluate the effects of TiO_2 exposure on the growth of RSV in mice, pulmonary viral titers were measured by plaque assay (Fig. 1). Viral titers of mice exposed to TiO_2 were not elevated significantly compared with those of control. Thus, TiO_2 exposure did not enhance proliferation of RSV in mice.

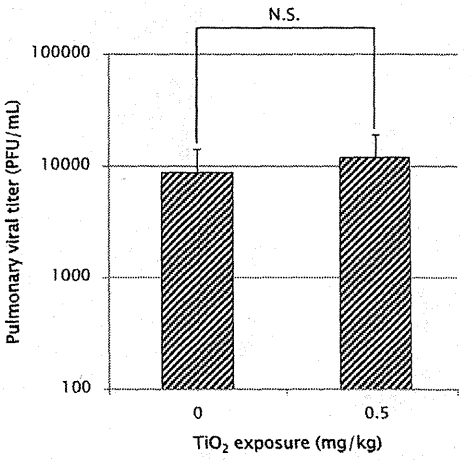

Fig. 1 – Effect of exposure to TiO_2 on pulmonary viral titers of RSV-infected mice on day 5 post-infection. The data represents mean ± standard deviation of values of 7 control or 5 TiO_2-treated mice. N.S., not significant.

3.2. *Effects of TiO_2 nanoparticles on severity of pneumonia in RSV infection*

To clarify the effects of TiO_2 nanoparticles on the severity of pneumonia in RSV infection, a histopathological assay was performed. In this experiment, 3–5 mice in each group were treated with TiO_2 as follows: a control group at 0 mg/kg, low-dose group at 0.25 mg/kg, and high-dose group at 2.5 mg/kg. These mice were infected with or without RSV 5 days after TiO_2 exposure. On day 5 post-infection, the mice were sacrificed, and their lung tissues were analyzed histopathologically. Representative results and changes in severity are presented in Fig. 2 and Table 4, respectively. In mock-infected mice, no obvious change in the lung tissues due to TiO_2 exposure was observed compared with the control (Fig. 2A-a, -c, and -e). In RSV-infected mice, typical features of pneumonia due to RSV infection, such as degeneration of the bronchial epithelium and infiltration of lymphocytes and neutrophils, were observed in mice treated with or without TiO_2 (Fig. 2A-b, -d, and -f). Severity of pneumonia was assessed as the proportion of alveolar septum tissue in RSV-infected mice (Table 4). In the control group at 0 mg/kg, the proportion of alveolar septa of all mice was less than 60%. On the other hand, two mice in the TiO_2 (0.25 mg/kg)-treated group had more than 60% alveolar septa, and one mouse in the TiO_2 (2.5 mg/kg)-treated group had more than 70%. The unit area means were 51.8%, 60.6%,

Table 3 – Effects of TiO_2 on levels of chemokines in BALF and serum of RSV-infected mice on day 5 post-infection.[a]

TiO_2 exposure (mg/kg)	Concentration in BALF (ng/mL)				Concentration in serum (ng/mL)	
	RSV-infected		Mock-infected		RSV-infected	Mock-infected
	CCL3	CCL5	CCL3	CCL5	CCL5	CCL5
0	0.10 ± 0.04	0.24 ± 0.06	<0.01	<0.01	0.14 ± 0.01	0.10 ± 0.01
0.5	0.11 ± 0.03	0.32 ± 0.07	<0.01	<0.01	0.18 ± 0.03*	0.09 ± 0.03

[a] Concentration (ng/mL) of each chemokine in BALF and serum from RSV-infected mice treated with or without TiO_2 (0.5 mg/kg) was measured by ELISA for each specific chemokine. Data represents mean values of 3–6 mice. Numbers in parentheses indicate standard deviation.
* Statistically different from control at $P < 0.05$ (Student's t-test).

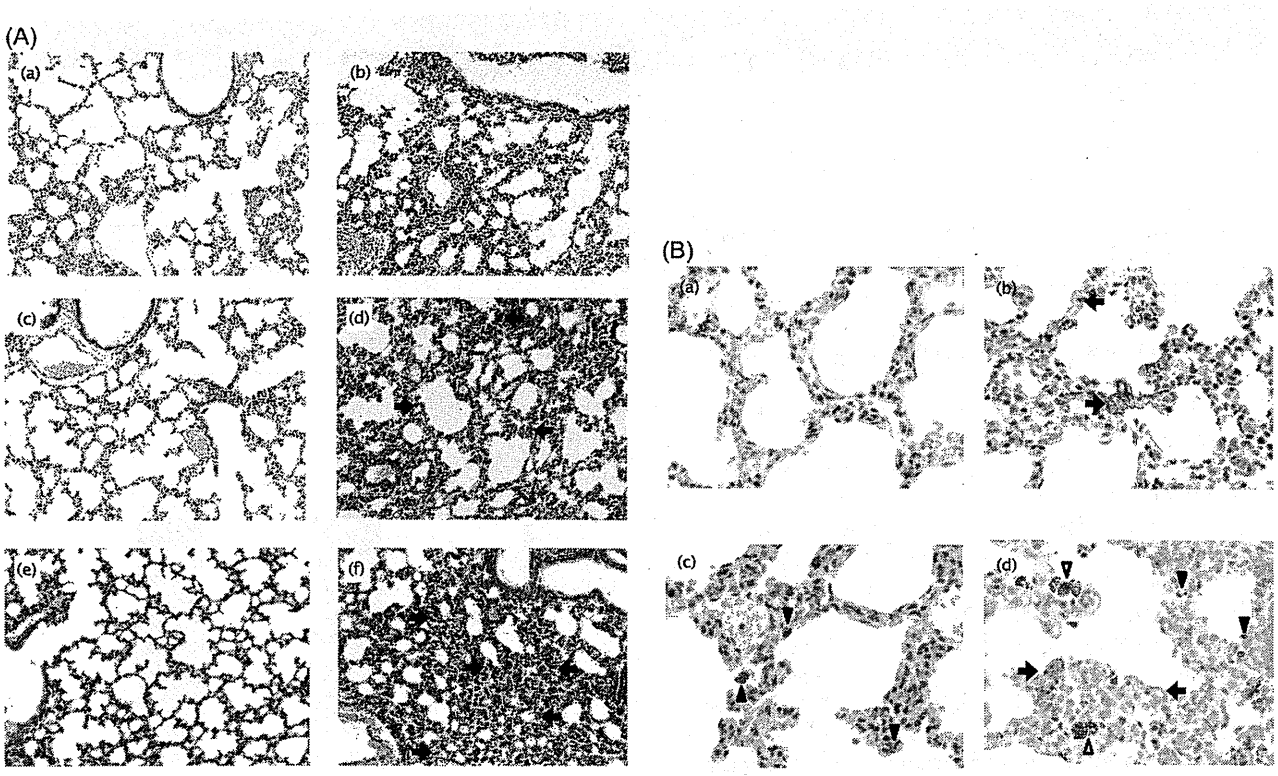

Fig. 2 – Lungs of mice 5 days after RSV-infection. (A) Hematoxylin and eosin staining (×100). (a) Control mouse with mock infection. (b) Control mouse with RSV infection. (c) TiO_2-treated (0.25 mg/kg) mouse with mock infection. (d) TiO_2-treated (0.25 mg/kg) mouse with RSV infection. (e) TiO_2-treated (2.5 mg/kg) mouse with mock infection. (f) TiO_2-treated (2.5 mg/kg) mouse with RSV infection. Arrows indicate infiltration of lymphocytes in alveolar septa. (B) Immunostained with anti-RSV protein antibodies (1:250) and counterstained with hematoxylin (×400). (a) Control mouse with mock infection. (b) Control mouse with RSV infection. (c) TiO_2-treated (2.5 mg/kg) mouse with mock infection. (d) TiO_2-treated (2.5 mg/kg) mouse with RSV infection. Closed arrows indicate RSV-positive cells, closed arrowheads indicate TiO_2 nanoparticles, and open arrowheads indicate aggregation of TiO_2 nanoparticles in inflammatory cells.

Table 4 – Effects of TiO_2 on proportion of tissue of alveolar septa in RSV-infected mice on day 5 post-infection.

TiO_2 exposure (mg/kg)	% of alveolar tissues[a]				% of mean alveolar tissues
	>40	>50	>60	>70	
0	2	2	0	0	51.8 (3.7)
0.25	0	2	2	0	60.6 (1.6)
2.5	0	0	1	1	68.6 (3.1)

[a] The proportion of tissue in alveolar septa per unit area by Adobe Photoshop.
* Number of mice. Numbers in parenthesis indicate the standard error.

Table 5 – Effects of TiO_2 on CCL3 production from bronchoalveolar lavage cells on day 1 post-infection in RSV-infected mice.

TiO_2 exposure (mg/mL)	CCL3 (ng/mL)[a]	
	−LPS	+LPS
0	<0.01	0.17 (0.12–0.23)*
0.1	<0.01	0.15 (0.13–0.16)

[a] Bronchoalveolar lavage cells were collected from RSV-infected mice and cultured for 48 h with or without TiO_2 (0.1 mg/mL).
* Data represent mean of values of two separate experiments. Numbers in parentheses indicate the range of values.

and 68.6% in each group, respectively. Thus, we confirmed exacerbation of the pneumonia due to RSV infection by TiO_2 exposure.

To investigate whether the distribution of RSV-infected cells was changed qualitatively due to TiO_2 (2.5 mg/kg) exposure, sections of the lung tissues of RSV-infected mice were stained immunohistochemically with a goat-polyclonal antibody against RSV protein (Fig. 2B). There was no significant change in the localization of RSV-positive cells, but the TiO_2 nanoparticles were not close to RSV-positive cells (Fig. 2B-b and -d). Similar results were observed for TiO_2 (0.25 mg/kg)-treated mice (data not shown). However, there was aggregation of TiO_2 nanoparticles near inflammatory cells in the severe region (Fig. 2B-d). Because these results suggested that TiO_2 nanoparticles might influence the function of macrophage/monocyte in an early phase of RSV infection, bronchoalveolar lavage cells on day 1 post-infection from RSV-infected mice were incubated for 48 h with or without 0.1 mg/mL of TiO_2, corresponding to a dose of 0.5 mg/kg *in vivo*. After incubation, the levels of CCL3 in the culture supernatant of the cells were measured by ELISA (Table 5). Although the cells were stimulated with LPS, there was no significant change in the production of CCL3 from bronchoalveolar lavage cells due to TiO_2 treatment.

4. Discussion

We assessed the effects of TiO_2 nanoparticles on the immune response using a mouse model of RSV infection (Watanabe et al., 2008a) and found that prior exposure to TiO_2 nanoparticles exacerbated pneumonia in the lungs of mice.

Various studies concerning risk assessment of TiO_2 nanoparticles in murine models have been reported (Chen et al., 2013; Kwon et al., 2012; Lindberg et al., 2012; Xu et al., 2010). In many cases, TiO_2 exposure was performed at a high dosage and/or multiple times. For example, to evaluate the carcinogenesis of TiO_2 nanoparticles in lung tissues, female (10 weeks old) SD rats were subjected to intra-pulmonary spraying five times with 0.5 mL suspensions of TiO_2 nanoparticles at 500 μg/mL in saline (Xu et al., 2010). In our assay, female (6 weeks old) BALB/c mice were exposed once intranasally to 0.1 mL of a suspension of TiO_2 nanoparticles at 50 μg/mL or 100 μg/mL, corresponding to a dose of 0.25 mg/kg or 0.5 mg/kg of body weight. The levels of TiO_2 exposure in our assay are much lower than those in previous studies (Chen et al., 2013; Kwon et al., 2012; Lindberg et al., 2012; Xu et al., 2010), and suppression of body weight, abnormal behavior, or dystrophy due to the stress of TiO_2 exposure was not observed compared with the control mice (data not shown). Furthermore, in the TiO_2-treated mice without RSV infection, no significant enhancement of cytokines or chemokines in BALF and any obvious changes in lung tissues were observed (Table 1, 3, Fig. 2A-a, -c, -e, B-a, and -c). Based on these experiments, we are confident that RSV infection is a useful tool for evaluation of the effects of low-level exposure to TiO_2 nanoparticles on the immune system, which was not reported previously.

The IFN-γ levels of RSV-infected mice treated with TiO_2 were enhanced significantly ($P < 0.05$) compared with the control (Table 1). These results suggest that pneumonia in RSV-infected mice was exacerbated due to TiO_2 exposure. However, viral titers in lung tissues of RSV-infected mice exposed to TiO_2 were not elevated significantly compared with the control (Fig. 1), and there was no significant increase of the number of RSV-positive cells in lung tissues due to TiO_2 exposure (Fig. 2B). Previous studies concerning evaluation of immunotoxicity of BFRs such as DBDE and TBBPA have shown that these compounds clearly increased both the levels of IFN-γ and viral titers in RSV-infected mice, resulting in the exacerbation of pneumonia (Watanabe et al., 2008b, 2010a,b). Therefore, we speculated that the mechanism of action of TiO_2 nanoparticles was different from that of BFRs on the immune system (Watanabe et al., 2008b, 2010a,b). We investigated further effects of exposure to TiO_2 on the Th1/2 balance of RSV-infected mice. The levels of IL-10, a Th2 cytokine, in BALF were increased significantly ($P < 0.05$) compared with the control (Table 1). IL-10 is produced mainly by T cells and acts by inhibiting the production of pro-inflammatory cytokines (Cavalcanti et al., 2012). Remarkably, although enhancement of the IL-10 levels should alleviate immune response, exacerbation of pneumonia was conversely exhibited (Fig. 2A). On the other hand, enhancement of IL-4 production due to TiO_2 exposure was not observed (Table 1). However, the levels of chemokine CCL5, an inflammatory marker called RANTES produced mainly by T cells and basophils (Schall et al., 1988), in BALF were also increased significantly ($P < 0.05$) compared with the control (Table 3). Thus, this irregular activation of T cells due to TiO_2 exposure might induce a Th1/2 imbalance. However, there was not a significant change in the population of IFN-γ-positive cells and IL-4-positive cells due to TiO_2 treatment by flow cytometric analysis (Table 2). These results suggested that TiO_2 exposure probably affected the secretion of the cytokines rather than differentiation of $CD4^+$ cells, responding to RSV infection.

In the histopathological analysis, the infiltration of lymphocytes in alveolar septa in RSV-infected mice tended to be increased by TiO_2 exposure, particularly in wide areas of lung tissues (Fig. 2A and Table 4). Because chemokine CCL5 promotes the migration of T cells and basophils (Schall et al., 1988), enhancement of it should contribute to the infiltration (Table 3). Moreover, in an immunohistochemical analysis, we observed TiO_2 nanoparticles explicitly because the sections were faintly counterstained with hematoxylin (Fig. 2B). It became evident that TiO_2 nanoparticles were aggregated by lymphocytes/macrophages but were not close to RSV-positive cells. It has been reported that TiO_2 nanoparticles were engulfed in alveolar macrophages and involved in the

inflammation in lung tissues of the TiO_2-treated rodents (Kwon et al., 2012; Xu et al., 2010). Then, to evaluate whether TiO_2 exposure influence the function of macrophages/monocytes in lung tissue of RSV-infected mice, the bronchoalveolar lavage cells on day 1 post-infection, consist mainly of the macrophage/monocyte-like cells (Watanabe et al., 2010a), were cultured with or without TiO_2 (Table 5). The *in vitro* experiment using a LPS showed that TiO_2 treatment did not affect the production of chemokine CCL3 from the bronchoalveolar lavage cells, although the ingestion of TiO_2 nanoparticles in the macrophage/monocyte-like cells was observed under a microscope. Therefore, further studies are needed to understand whether macrophages are involved in the immune response in an early phase of RSV infection.

TiO_2 nanoparticles are used in various products, and we may be exposed to them at various times of life. We have already confirmed that anatase crystals of TiO_2 nanoparticles used in building materials induced the elevation of CCL5 in RSV-infected mice (data not shown). In this study, we used TiO_2 nanoparticles that form rutile crystals and are used in cosmetics. Further studies are required to investigate the effects of TiO_2 nanoparticles of different forms and sizes on immune response. These studies should provide useful information to manage their effects on health, including methods of skin care.

Conflict of interests

The authors declare that they have no conflict of interests.

Acknowledgments

The authors thank Dr. Masaki Umeda (Vpec, Tokyo, Japan) who stained and evaluated lung tissues. We also thank Katherine Ono for editing the paper. This study was supported by a Health and Labour Sciences Research Grant (H24-kagaku-shitei-009) from the Ministry of Health, Labour and Welfare, Japan and partly by grant-in-Aid for Science Research (No. 26460183) from the Japan Society for the Promotion of Science.

REFERENCES

Cavalcanti, Y.V., Brelaz, M.C., Neves, J.K., Ferraz, J.C., Pereira, V.R., 2012. Role of TNF-alpha, IFN-gamma, and IL-10 in the development of pulmonary tuberculosis. Pulm. Med. 2012, 745483.

Chen, T., Hu, J., Chen, C., Pu, J., Cui, X., Jia, G., 2013. Cardiovascular effects of pulmonary exposure to titanium dioxide nanoparticles in ApoE knockout mice. J. Nanosci. Nanotechnol. 13, 3214–3222.

Collins, P.L., Chanock, R.M., Murphy, B.R., 2001. Respiratory syncytial virus. In: Knipe, D.M., Howley, P.M. (Eds.), Fields Virology. Lippincott Willams & Wilkins, Philadelphia, PA, pp. 1443–1485.

Falsey, A.R., 2007. Respiratory syncytial virus infection in adults. Semin. Respir. Crit. Care Med. 28, 171–181.

Falsey, A.R., Hennessey, P.A., Formica, M.A., Cox, C., Walsh, E.E., 2005. Respiratory syncytial virus infection in elderly and high-risk adults. N. Engl. J. Med. 352, 1749–1759.

Holberg, C.J., Wright, A.L., Martinez, F.D., Ray, C.G., Taussig, L.M., Lebowitz, M.D., 1991. Risk factors respiratory syncytial virus-associates lower respiratory illnesses in the first year of life. Am. J. Epidemiol. 133, 1135–1151.

Huerta-Garcia, E., Pérez-Arizti, J.A., Márquez-Ramírez, S.G., Delgado-Buenrostro, N.L., Chirino, Y.I., Iglesias, G.G., López-Marure, R., 2014. Titanium dioxide nanoparticles induce strong oxidative stress and mitochondrial damage in glial cells. Free Radic. Biol. Med. 73, 84–94.

Kwon, S., Yang, Y.S., Yang, H.S., Lee, J., Kang, M.S., Lee, B.S., Lee, K., Song, C.W., 2012. Nasal and pulmonary toxicity of titanium dioxide nanoparticles in rats. Toxicol. Res. 28, 217–224.

Lambert, A.L., Trasti, F.S., Mangum, J.B., Everitt, J.I., 2003. Effects of preexposure to ultrafine carbon black on respiratory syncytial virus infection in mice. Toxicol. Sci. 72, 331–338.

Lindberg, H.K., Flack, G.C., Catalán, J., Koivisto, A.J., Suhonen, S., Järventaus, H., Rossi, E.M., Nykäsenoja, H., Peltonen, Y., Moreno, C., Alenius, H., Tuomi, T., Savolainen, K.M., Norppa, H., 2012. Genotoxicity of inhales nanosized Ti0(2) in mice. Mutat. Res. 745, 58–64.

MacDonald, N.E., Hall, C.B., Suffin, S.C., Alexson, C., Harris, P.J., Manning, J.A., 1982. Respiratory syncytial viral infection in infants with congenital heart disease. N. Engl. J. Med. 307, 397–400.

Maidalawieh, A., Kanan, M.C., E.I-Kadri, O., Kanan, S.M., 2014. Recent advances in gold and silver nanoparticles: synthesis and applications. J. Nanosci. Nanotechnol. 14, 4547–4580.

Nel, A., Xia, T., Mädler, L., Li, N., 2006. Toxic potential of materials at the nanolevel. Science 311, 622–627.

Schall, T.J., Jongstra, J., Dyer, B.J., Jorgensen, J., Clayberger, C., Davis, M.N., Krensky, A.M., 1988. A human T cell-specific molecule is a member of a new gene family. J. Immunol. 141, 1018–1025.

Stamatoiu, O., Mirzaei, J., Feng, X., Hegmann, T., 2012. Nanoparticles in liquid crystals and liquid crystalline nanoparticles. Top. Curr. Chem. 318, 331–393.

Takeda, S., Hidaka, M., Yoshida, H., Takeshita, M., Kikuchi, Y., Tsend-Ayush, C., Dashnyam, B., Kawahara, S., Muguruma, M., Watanabe, W., Kurokawa, M., 2014. Antiallergic activity of probiotics from Mongolian dairy products on type I allergy in mice and mode of antiallergic action. J. Funct. Foods 9, 60–69.

Takeshita, T., Watanabe, W., Toyama, S., Hayashi, Y., Honda, S., Sakamoto, S., Matsuoka, S., Yoshida, H., Takeda, S., Hidaka, M., Tsutsumi, S., Yasukawa, K., Park, Y.K., Kurokawa, M., 2013. Effects of Brazilian propolis on exacerbation of respiratory syncytial virus infection in mice exposed to tetrabromobisphenol a, a brominated flame retardant. Evid. Based Complement. Altern. Med. 2013, 698206.

Watanabe, W., Shimizu, T., Hino, A., Kurokawa, M., 2008a. A new assay system for evaluation of developmental immunotoxicity of chemical compounds using respiratory syncytial virus infection to offspring mice. Environ. Toxicol. Pharmacol. 25, 69–74.

Watanabe, W., Shimizu, T., Hino, A., Kurokawa, M., 2008b. Effects of decabrominated diphenyl ether (DBDE) on developmental immunotoxicity in offspring mice. Environ. Toxicol. Pharmacol. 26, 315–319.

Watanabe, W., Shimizu, T., Sawamura, R., Hino, A., Konno, K., Kurokawa, M., 2010a. Functional disorder of primary immunity responding to respiratory syncytial virus infection in offspring mice exposed to a flame retardant, decabrominated dephenyl ether, perinatally. J. Med. Virol. 82, 1075–1082.

Watanabe, W., Shimizu, T., Sawamura, R., Hino, A., Konno, K., Hirose, A., Kurokawa, M., 2010b. Effects of tetrabromobisphenol A, a brominated flame retardant, on the immune response to respiratory syncytial virus infection in mice. Int. Immunopharmacol. 10, 393–397.

Watanabe, W., Yoshida, H., Hirose, A., Akashi, T., Takeshita, T., Kuroki, N., Shibata, A., Hongo, S., Hashiguchi, S., Konno, K., Kurokawa, M., 2013. Perinatal exposure to insecticide methamidophos suppressed production of proinflammatory cytokines responding to virus infection in lung tissues in mice. Biomed. Res. Int., 151807.

Xu, J., Futakuchi, M., Iigo, M., Fukamachi, K., Alexander, D.B., Shimizu, H., Sakai, Y., Furukawa, F., Uchino, T., Tokunaga, H., Nishimura, T., Hirose, A., Kanno, J., Tsuda, H., 2010. Involvement of macrophage inflammatory protein 1 alpha (MIP1alpha) in promotion of rat lung and mammary carcinogenic activity of nanoscale titanium dioxide particles administered by intra-pulmonary spraying. Carcinogenesis 31, 927–935.

Zhang, H., Wang, C., Chen, B., Wang, X., 2012. Daunorubicin-TiO_2 nanocomposites as a smart pH-responsive drug delivery system. Int. J. Nanomed. 7, 235–242.

The Journal of Toxicological Sciences (J. Toxicol. Sci.)
Vol.39, No.3, 499-505, 2014

Original Article

MWCNT causes extensive damage to the ciliated epithelium of the trachea of rodents

Teruya Ohba[1], Jiegou Xu[2], David B. Alexander[2], Akane Yamada[1], Jun Kanno[3], Akihiko Hirose[4], Hiroyuki Tsuda[2] and Yuji Imaizumi[1]

[1]*Department of Molecular and Cellular Pharmacology, Nagoya City University Graduate School of Pharmaceutical Sciences, 3-1 Tanabedori, Mizuhoku, Nagoya 467-8603, Japan*
[2]*Laboratory of Nanotoxicology, Nagoya City University, 3-1 Tanabedori, Mizuhoku, Nagoya 467-8603, Japan*
[3]*Division of Cellular and Molecular Toxicology, 1-18-1 Kamiyoga, Setagaya-ku, Tokyo 158-8501, Japan*
[4]*Division of Risk Assessment, National Institute of Health Sciences, 1-18-1 Kamiyoga, Setagaya-ku, Tokyo 158-8501, Japan*

(Received February 19, 2014; Accepted April 8, 2014)

ABSTRACT — The ciliated tracheobronchial epithelium plays an important role in the excretion of inhaled dust. While many reports indicate that inhaled multi-walled carbon nanotubes (MWCNT) induce inflammation and proliferative changes in the lung and pleura, their effects on the upper airway have not been reported. Two different types of MWCNTs, MWCNT-L (8 μm in length and 150 nm in diameter) and MWCNT-S (3 μm in length and 15 nm in diameter), were examined for their effect on the trachea as well as the bronchus and lung. *In vitro*, the movement of the cilia of primary tracheal epithelial cells was impaired by treatment with the 2 MWCNTs. Rats were treated with 0.3 ml of a 250 μg/ml suspension of MWCNTs on days 1, 4, and 7, and sacrificed on day 8. Extensive loss of ciliated cells and replacement by flat cells without cilia was observed in the trachea. Deposition of MWCNTs and occasional squamous cell metaplasia were found in the regenerative granulation tissue. The proportion of the lesion to the transverse section of the trachea was vehicle, 0; MWCNT-L, 27.2 ± 10.5; MWCNT-S, 32.1 ± 15.8 (both MWCNTs, $p < 0.001$ vs vehicle). The amount of cilia showed significant decrease in the MWCNT-L treated rats ($p < 0.05$). In contrast to the trachea lesions, the number of inflammatory foci in the lung was greater in the MWCNT-S than in the MWCNT-L treated rats. Our results indicate that both MWCNTs caused extensive damage to the ciliated epithelium of the trachea. This damage may prolong the deposition of inhaled MWNCT in the lung.

Key words: MWCNT, Tracheal damage, Ciliated epithelium, Rat

INTRODUCTION

Multi-walled carbon nanotubes (MWCNT) are a newly developed material with potential applications in many fields including the biomedical field. The high aspect ratio of MWCNT is similar to that of asbestos and has led to concern that exposure to MWCNT might cause asbestos-like lung diseases (Bonner, 2010; Donaldson *et al.*, 2010; Nagai and Toyokuni, 2010). Many reports have indicated that exposure of rats to MWCNT induces inflammation, fibrosis and oxidative stress in the lung and pleura (Mercer *et al.*, 2010, 2013; Xu *et al.*, 2012). To date, *in vivo* studies have focused on the toxicity of MWCNT in the lung and pleura, and nothing has been reported regarding the effect of MWCNT on the epithelium of the trachea.

The tracheal and primary branch of the bronchial epithelium is mainly composed of ciliated cells and some goblet cells. The ciliated cells are responsible for carrying out inhaled dust particles in the throat by their ciliary transportation movement. Thus, the ciliated cells play a pivotal role in the defense of the airway against inhaled particle matter. Several environmental factors such as cigarette smoke (Simet *et al.*, 2010) and diesel gas particles (Li *et al.*, 2011) have been shown to impair ciliated cell functions, resulting in increased pulmonary deposition. Zinc oxide nanoparticles have been reported to induce proliferation of airway epithelial cells and goblet cell hyperplasia (Cho *et al.*, 2011) and transient epithelial hyperplasia of the terminal bronchiole (Xu *et al.*,

Correspondence: Yuji Imaizumi (E-mail: yimaizum@phar.nagoya-cu.ac.jp)

2014). Although several reports indicate that MWCNT have some toxic effects on bronchial epithelial cells *in vitro* (Hirano *et al.*, 2010; Lindberg *et al.*, 2009; Rotoli *et al.*, 2008), the effect on the upper airway in animals remains unknown. In the present study, we investigated the effects of MWCNT on the tracheal epithelium *in vitro* and *in vivo* and the bronchus and lung *in vivo* after short-term exposure.

MATERIALS AND METHODS

Animals

8-12 week old C57BL/6N male mice (Japan SLC Inc., Shizuoka, Japan) and 6-7 week old Wistar/ST rats were obtained from Japan SLC Inc. Rats were housed in the Animal Center of Nagoya City University Graduate School of Pharmaceutical Sciences and maintained on a 12 hr light/12 hr dark cycle and received Oriental MF basal diet (Oriental Yeast Co. Ltd., Tokyo, Japan) and water *ad libitum*. The study was conducted according to the Guidelines for the Care and Use of Laboratory Animals of Nagoya City University Graduate School of Pharmaceutical Sciences, and the experimental protocol was approved by the Nagoya City University Animal Care and Use Committee (H24-p-12).

Preparation of MWCNT and Fluorescent Microspheres (FMS)

We used two types of MWCNTs, MWCNT-L and MWCNT-S, which are grown in the vapor phase. According to the manufacturer's information, the primary size of MWCNT-L is 150 nm in mean diameter and 8 μm in mean length, and the primary size of MWCNT-S is 15 nm in mean diameter and 3 μm in mean length. Five milligrams of MWCNT-L or MWCNT-S were suspended in 20 ml of saline containing 0.5% Pluronic F68 (PF68, non-ionic, biocompatible amphiphillic block copolymers, Sigma-Aldrich, St Louis, MO, USA) and homogenized for 1 min at 3,000 rpm in a Polytron PT1600E benchtop homogenizer (Kinematika AG, Littau, Switzerland) 4 times. The suspensions were sonicated for 30 min shortly before use to minimize aggregation. The concentration of the MWCNTs was 250 μg/ml. Both MWCNT-L and MWCNT-S dispersed well in the vehicle solution. MWCNT-L showed single fibers with a needle-like shape under scanning electron microscope (SEM) observation, but gradually formed agglomerates over time. Since MWCNT-S are tangled fibers, it showed cotton-like aggregation in suspension under SEM observation. However, they did not form larger agglomerates: incubation in suspension up to 7 days (data not shown). Fluorescent Microspheres (FMS) were purchased from Invitrogen (TetraSpeckTM microspheres, 500 nm in diameter) and suspended by sonication at 250 μg/ml in saline containing 0.5% PF68.

Isolation of single ciliated cells

Isolation of single ciliated cells was as previously reported (Ma *et al.*, 2006). Briefly, the tracheal epithelium was separated from the cartilage and cut into pieces of approximately 0.1 × 0.1 cm. The tissue was incubated in phosphate-buffered saline containing NaCl 137 mM, KCl 2.7 mM, $CaCl_2$ 0.9 mM, $MgCl_2$ 0.5 mM, Na_2HPO_4 8 mM, KH_2PO_4 1.47 mM and d-glucose 5 mM, pH 7.4 (PBS-g) supplemented with 13 U/ml papain (Sigma), 1 mg/ml bovine serum albumin (Sigma-Aldrich) and 1 mg/ml 1,4-dithiothreitol (Wako Chemicals Co. Ltd., Osaka, Japan). Cells were then dispersed several times with a fire-polished Pasteur pipette and re-suspended in PBS-g and used immediately.

In vitro study

The isolated mouse tracheal epithelial cells were maintained in high glucose Dulbecco's modified Eagle's medium (DMEM, Sigma) supplemented with 10% fetal bovine serum (FBS), 1 U/ml penicillin G, and 0.1 mg/ml streptomycin sulfate, at 37°C, 5% CO_2. The cells were then exposed for 10 min to vehicle, FMS, MWCNT-L, or MWCNT-S in FMS or MWCNT suspensions to a final concentration of 10 μg/ml. Media was then replaced by fresh media. The cells were observed 10 min and 12 and 18 hr after addition of fresh media and the proportion of cells with ciliary movement per total ciliated cells was determined. For each group, approximately 500 cells per dish in three separate dishes were counted.

Rat study

Male Wistar rats aged 6-7 weeks were treated with 0.3 ml of 250 μg/ml MWCNT-L or MWCNT-S (3 rats each) suspended in PF68 vehicle on days 1, 4, and 7. The suspension was administered by a microsprayer (series 1A-1B Intratracheal Aerosolizer; Penn-century, Philadelphia, PA, USA) with the tip of the microsprayer just inside the entrance of the trachea (Xu *et al.*, 2012). Administration was done in synchronization with spontaneous inhalation. The rats were sacrificed 24 hr after the last dosing (day 8) under deep anesthesia with isoflurane. The trachea, bronchus and lung were excised and fixed in 4% paraformaldehyde solution. The trachea was transversely cut into 3 pieces, upper, middle and lower parts, and the tracheal sections and the bronchus and lungs were routinely processed for paraffin embedding, sectioning and histological examination.

Histology and Immunostaining

Haematoxylin-Eosin (H&E) stained slides of the trachea; bronchus and lung were examined by board pathologists. The epithelial lesions in each tracheal section were measured with the image analyzing function (Nikon, Tokyo, Japan) and expressed as the ratio of the length of the lesion to the whole length of the tracheal section. The number of granulation foci of the lung sections were counted and expressed as number/cm^2 lung tissue. Localization of MWCNT fibers in the trachea and lung tissue were determined with polarized light microscopy (Olympus BX51N-31P-O, Tokyo, Japan) at × 400 and × 1,000 magnification. Immunostaining of acetyled tublin, a specific marker for cilia, was performed using mouse polyclonal anti-acetyled tublin antibody (Sigma Aldrich). The antibody was diluted 1:1,000 in PBS containing 5% goat albumin and applied to deparaffinized and blocked slides, and the slides were incubated at 4°C overnight. The next day, the slides were washed 3 times in PBS and then incubated for 2 hr with Alexa 488-conjugated goat anti-mouse IgG (Molecular Probe, Eugene, OR, USA) diluted 1:1,000. After washing 3 times in PBS, the slides were counterstained with DAPI (Vector laboratories, Burlingame, CA, USA). Immunostained sections were observed using an A1R laser scanning confocal microscope (Nikon). The ratio of the fluorescent intensity of acetyled tublin in the top layer of cells of the tracheal ciliated epithelium to the fluorescent intensity of DAPI in the underlying submucosal tissue was measured. This ratio was used to compare the intensity of acetyled tublin fluorescence in the different samples. Fluorescence intensity was determined with NIS Elements software (version 3.10; Nikon).

Statistical Analysis

Statistical significance was examined using Tukey's test. P values less than 0.05 were considered to be statistically significant.

RESULTS

In vitro study

Cultures of ciliated cells were incubated in growth media with vehicle (PF68), fluorescent microspheres (FMS), or MWCNT for 10 min. During the 10 min incubation in media containing FMS, FMS in contact with the cilia and/or cell surface could readily be located (white arrow in Fig. 1A in bottom panel), however, 10 min after replacing the FMS containing media with standard growth media, cell-associated FMS could no longer be found. In contrast, ten min after replacing the MWCNT containing media with standard growth media, MWCNT-L and MWCNT-S fibers were not detached from the ciliated cells and could be observed associated with the cilia and/or cell surface (black arrows in Fig. 1A). In the cilia activity test, FMS did not reduce the percentage of cells with active cilia compared to the vehicle group (Fig. 1B). However, the percentage of cells with active cilia in the MWCNT-L treated group was significantly reduced (2.73 ± 1.37; n = 3, $p < 0.05$) compared to the vehicle (18.7 ± 4.28) and FMS (16.57 ± 0.65) groups after 12 hr. Although not significant, a similar decrease was also observed in the MWCNT-S group.

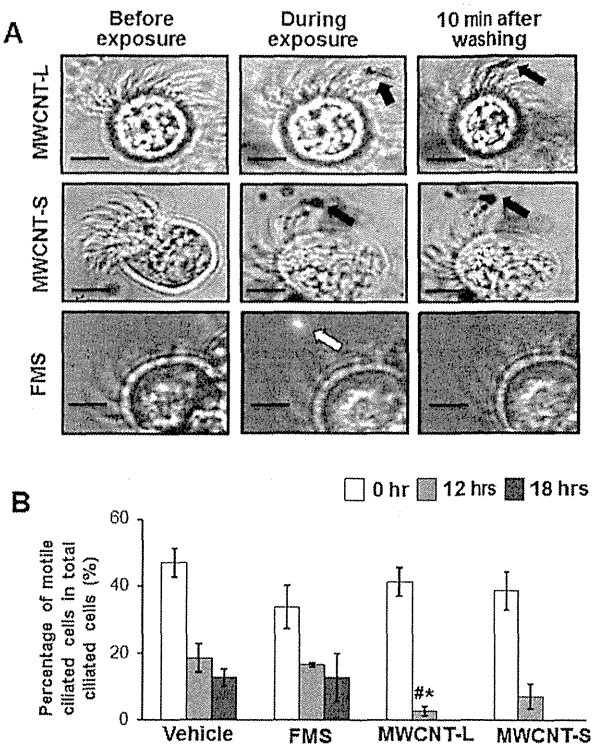

Fig. 1. Exposure of MWCNT to isolated tracheal ciliated cells *in vitro*. A, Images of ciliated cells exposed to fluorescent microsphere (FMS), MWCNT-L, and MWCNT-S; left, before exposure; middle, during exposure; right, after media change. FMS (white arrow) was clearly removed. MWCNTs were not removed (black arrows). Bars equal 5 μm. B, Percentage of cells with active cilia at time 0 and 12 and 18 hr after media change. n = 3; * $p < 0.05$ vs vehicle control, # $p < 0.05$ vs FMS control.

Rat study

The majority of the epithelium of the trachea is com-

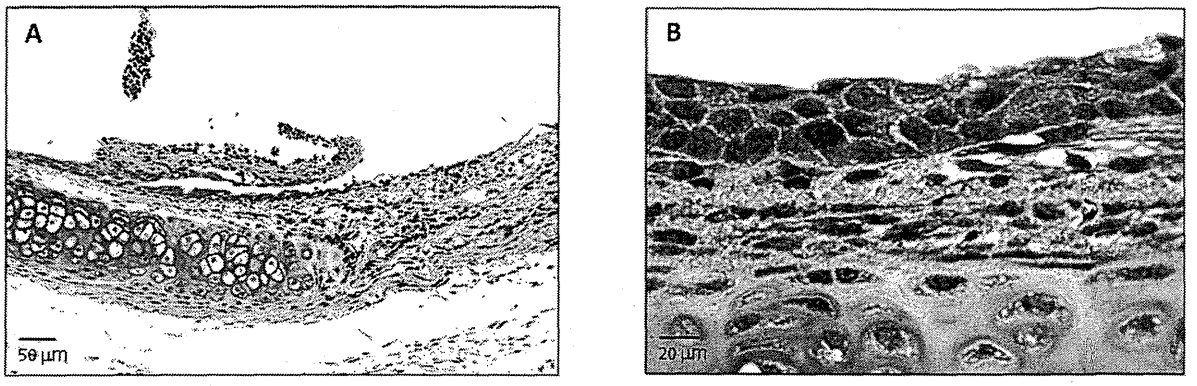

Fig. 2. Erosive lesions and squamous cell metaplasia. A, Representative image showing erosive lesions induced by treatment of MWCNT-L or MWCNT-S; B, Representative image of squamous cell metaplsia.

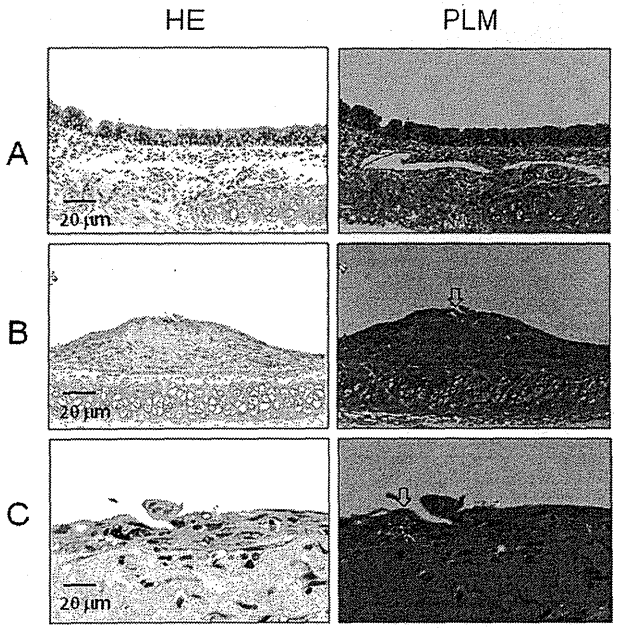

Fig. 3. Tracheal lesions in rat treated with MWCNT-L. A, Undamaged tracheal ciliated epithelium; B, An erosive lesion with granulation tissue underneath the thin regenerating epithelium; C, A higher magnification image of the lesion in B. MWCNT-L fibers (open arrows) can be clearly observed in the granulation tissue by polarized light microscopy (PLM).

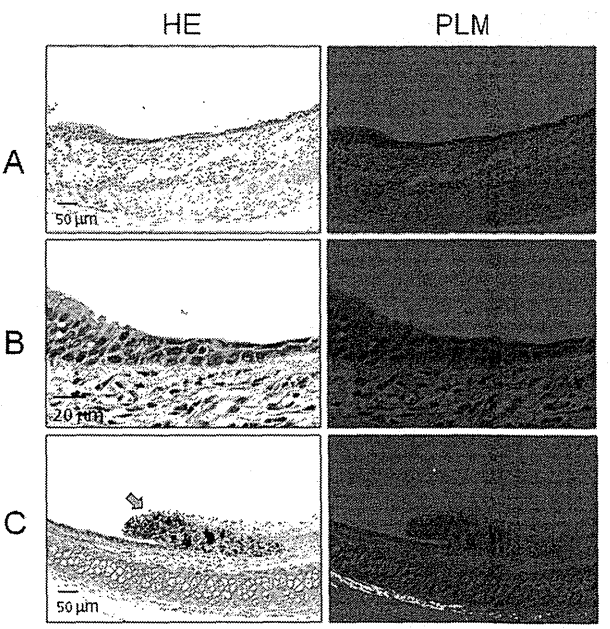

Fig. 4. Tracheal lesions in a rat treated with MWCNT-S. A, Tracheal epithelium showing a transition from undamaged ciliated epithelium to regenerating flat epithelium overlying edematous granulation tissue. B, A higher magnification image of the lesion in B. C, An erosive lesion with granulation tissue containing many black MWCNT-S fibers. MWCNT-S fibers are not visualized by polarized light microscopy (PLM).

posed of a single layer of columnar ciliated cells. Treatment with MWCNT-L induced marked damage to the surface ciliated cells resulting in erosive changes (Fig. 2A) and replacement with flat cells without cilia and occasional squamous cell metaplasia (Fig. 2B). An increase in goblet cells was found in the columnar ciliated cell area, although goblet cell damage was not obvious. MWCNT-L fiber aggregates were frequently observed in the lesions (Figs. 3B and 3C) but not in the healthy mucosa (Fig. 3A). MWCNT-S caused similar mucosal damage (Fig. 4,

Table 1. Lesions in the tracheal epithelium and lung

Treatment	No. of rats	Tracheal epithelium			Lung
		Erosion	Regenerated cells		
		Incidence (%)	Incidence (%)	Proportion [a] (%)	Granulation tissue (No./cm²) [b]
Vehicle	4	0	0	0	0
MWCNT-L	3	100 ***	100 ***	27.2 ± 8.7**	0.1 ± 0.1
MWCNT-S	4	25 ***	100 ***	32.7 ± 11.5**	1.0 ± 0.2 **,##

Notes: [a], the length of the regenerated lesion compared to the total length of the transverse tracheal circle; [b], the number of granulation lesions per square centimeter of the lung tissue; ** and *** represent p values < 0.01 and 0.001, vs the vehicle; ## represents p values < 0.01, vs MWCNT-L

left panel) but, because of lack of MWCNT-S mediated polarization, the fibers could not be detected by polarized light microscopy (Fig. 4C, right panel).

Table 1 shows the incidences of erosion and incidences and the percentage of the length of the tracheal lesions compared to the total length of the tracheal cross section from rats administered vehicle or MWCNT. Tracheal lesions in rats administered MWCNT-L (27.2 ± 10.5) or MWCNT-S (32.1 ± 15.8) were significantly greater than in rats administered vehicle alone ($p < 0.001$ for both comparisons). Although not significant, the incidences of erosive lesions for MWCNT-L administered rats was greater than for MWCNT-S administered rats.

The ratio of fluorescence of acetyled tublin on the surface of the trachea (0.48 ± 0.06) to submucosal DAPI fluorescence significantly decreased ($p < 0.05$) in rats treated with MWCNT-L (Fig. 5). The value for the MWCNT-S treated rats showed a similar decrease but was not significant. The results clearly indicate the quantitative loss of ciliated cells by treatment with MWCNT-L.

In the lung, granulation foci composed of macrophages and fibrotic cells surrounding MWCNT aggregates was found (Fig. 6). Table 1 shows the number of granulation foci in the lungs of rats administered vehicle or MWCNT. The number of lesions in both the MWCNT-L and MWCNT-S administered groups were significantly higher than in the vehicle control group ($p < 0.001$ for both comparisons). The lesion count in the MWCNT-S group (1.04 ± 0.18) was significantly greater than the MWCNT-L group (0.06 ± 0.06) ($p < 0.05$) (Table 1).

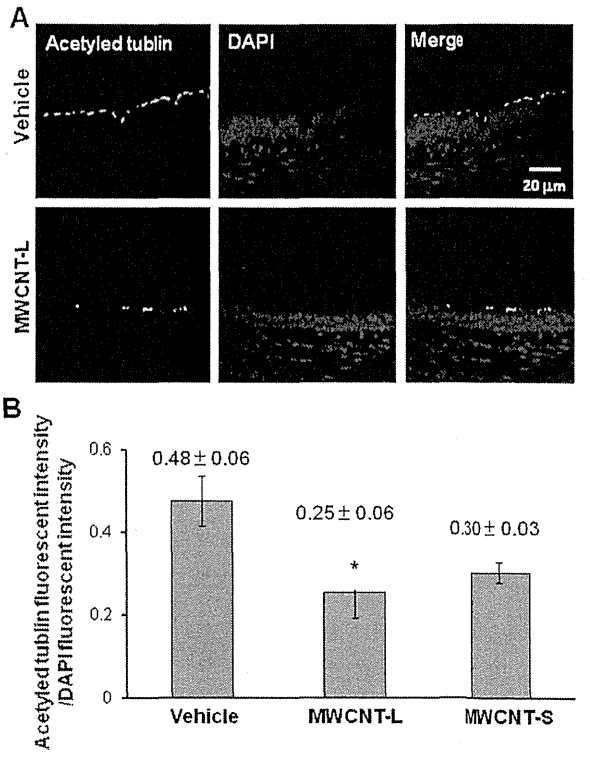

Fig. 5. Decrease in the proportion of ciliated cells in the bronchial epithelium. A, Representative images of immunostaining with anti-acetylated tubulin staining the cilia (left), DAPI (middle) and merged image (right); B, The ratio of the intensity of acetyled tublin to DAPI was decreased in the MWCNT-L group. n = 3~4; * $p < 0.05$ vs the vehicle.

DISCUSSION

The tracheobronchial ciliated epithelium is the first defense line against inhaled dust particles. The dust particles are transported from the lung alveoli through the bronchi and trachea toward the laryngopharynx by its directed ciliary movement. Pathologic changes in the bronchial epithelium such as goblet cell hyperplasia and squamous cell metaplasia have been found by studies

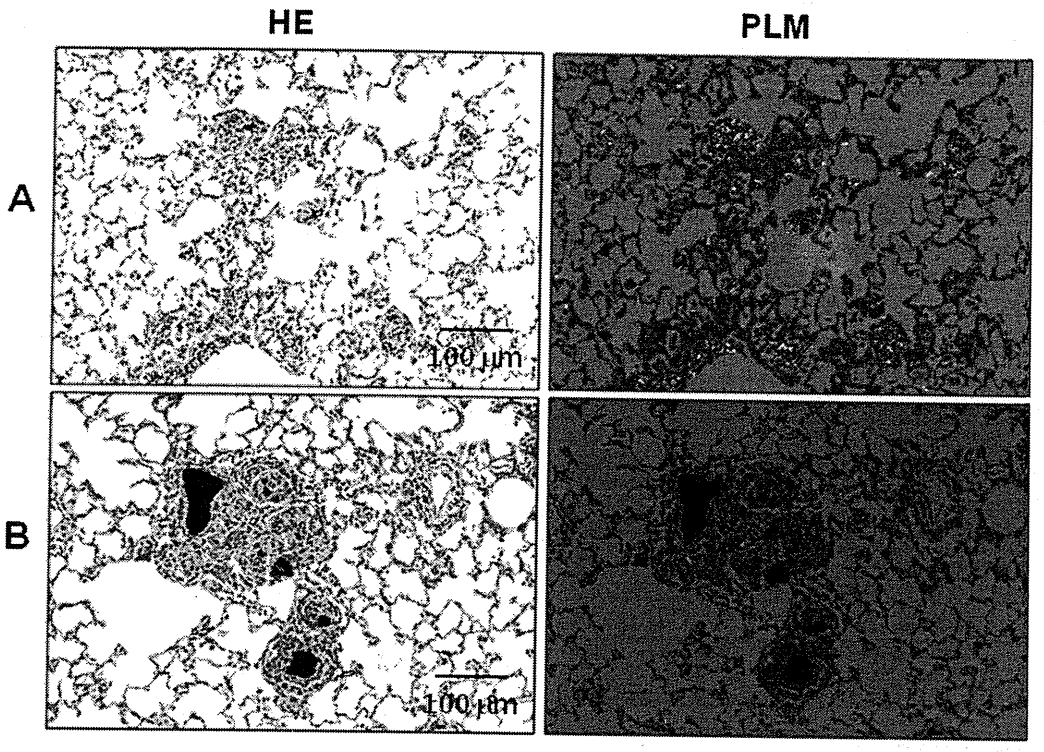

Fig. 6. Demonstration of MWCNTs in the lung tissue. HE and polarized images of the lung tissue treated with MWCNT-L (A) or MWCNT-S (B). Large aggregations of MWNNT-S (black mass) are found encapsulated in granulation tissue and small particles are found in alveolar macrophages. As in the trachea, MWCNT-S is not visualized by polarized light microscopy (PLM).

with particles such as ZnO particles (Choe *et al.*, 1997) and cigarette smoke (Neugut, 1988) and in some disease conditions such as bronchial asthma and chronic bronchitis (Aikawa *et al.*, 1992). The ciliated cell damage in these lesions causes impaired mucociliary protection and increases deposition of particles and microorganisms in the lung, causing inflammatory changes. These alterations may cause chronic injury and cell regeneration leading to an increase in carcinogenesis in the trachea, bronchi and lung.

This is the first report to show that MWCNTs cause extensive damage and loss of ciliated epithelium in the trachea followed by compensatory regeneration of cells without cilia including metaplastic squamous cells. *In vitro* observation clearly indicated that MWCNT caused impaired function of ciliated cells, potentially resulting in decreased clearance of the fibers from the lung, such as observed in studies of other fibers such as asbestos (Woodworth *et al.*, 1983). Decreased clearance of MWCNT would increase the retention time of the MWCNTs in the trachea and lung, which, in turn, would maintain the toxic effect, leading to even more loss of ciliated cells. This would increase the risk of spread of MWCNT to other organs, especially to the pleural cavity.

It should be noted that damage to the lung differed in MWCNT-L and MWCNT-S administered rats. Inflammatory changes, as evinced by an increase in granulation tissue in the lung, were more extensive in MWCNT-S administered rats. This indicates that there is an organotropic toxic effect of MWCNT. This may be related to their size and shape; however, further studies are necessary to elucidate the mechanism of this difference.

AKNOWLEDGMENTS

This study was supported by Grants-in-Aids by the Ministry of Health, Labour and Welfare, Japan: Risk of Chemical Substance 21340601 (H22-kagaku-ippan-005) and 2524301 (H25-kagaku-ippan-004).

REFERENCES

Aikawa, T., Shimura, S., Sasaki, H., Ebina, M. and Takishima, T. (1992): Marked goblet cell hyperplasia with mucus accumulation in the airways of patients who died of severe acute asthma attack. Chest, **101**, 916-921.

Bonner, J.C. (2010): Nanoparticles as a potential cause of pleural and interstitial lung disease. Proc. Am. Thorac. Soc., **7**, 138-141.

Cho, W.S., Duffin, R., Howie, S.E., Scotton, C.J., Wallace, W.A., Macnee, W., Bradley, M., Megson, I.L. and Donaldson, K. (2011): Progressive severe lung injury by zinc oxide nanoparticles; the role of Zn2+ dissolution inside lysosomes. Part Fibre. Toxicol., **8**, 27.

Choe, N., Tanaka, S., Xia, W., Hemenway, D.R., Roggli, V.L. and Kagan, E. (1997): Pleural macrophage recruitment and activation in asbestos-induced pleural injury. Environ. Health Perspect., **105 Suppl. 5**, 1257-1260.

Donaldson, K., Murphy, F.A., Duffin, R. and Poland, C.A. (2010): Asbestos, carbon nanotubes and the pleural mesothelium: a review of the hypothesis regarding the role of long fibre retention in the parietal pleura, inflammation and mesothelioma. Part. Fibre. Toxicol., **7**, 5.

Hirano, S., Fujitani, Y., Furuyama, A. and Kanno, S. (2010): Uptake and cytotoxic effects of multi-walled carbon nanotubes in human bronchial epithelial cells. Toxicol. Appl. Pharmacol., **249**, 8-15.

Li, J., Kanju, P., Patterson, M., Chew, W.L., Cho, S.H., Gilmour, I., Oliver, T., Yasuda, R., Ghio, A., Simon, S.A. and Liedtke, W. (2011): TRPV4-mediated calcium influx into human bronchial epithelia upon exposure to diesel exhaust particles. Environ. Health Perspect., **119**, 784-793.

Lindberg, H.K., Falck, G.C., Suhonen, S., Vippola, M., Vanhala, E., Catalan, J., Savolainen, K. and Norppa, H. (2009): Genotoxicity of nanomaterials: DNA damage and micronuclei induced by carbon nanotubes and graphite nanofibres in human bronchial epithelial cells *in vitro*. Toxicol. Lett., **186**, 166-173.

Ma, W., Korngreen, A., Weil, S., Cohen, E.B., Priel, A., Kuzin, L., and Silberberg, S.D. (2006): Pore properties and pharmacological features of the P2X receptor channel in airway ciliated cells. J. Physiol., **571**, 503-517.

Mercer, R.R., Hubbs, A.F., Scabilloni, J.F., Wang, L., Battelli, L.A., Schwegler-Berry, D., Castranova, V. and Porter, D.W. (2010): Distribution and persistence of pleural penetrations by multi-walled carbon nanotubes. Part. Fibre. Toxicol., **7**, 28.

Mercer, R.R., Scabilloni, J.F., Hubbs, A.F., Wang, L., Battelli, L.A., McKinney, W., Castranova, V. and Porter, D.W. (2013): Extrapulmonary transport of MWCNT following inhalation exposure. Part. Fibre. Toxicol., **10**, 38.

Nagai, H. and Toyokuni, S. (2010): Biopersistent fiber-induced inflammation and carcinogenesis: lessons learned from asbestos toward safety of fibrous nanomaterials. Arch. Biochem. Biophys., **502**, 1-7.

Neugut, A.I. (1988): Squamous cell cancers and cigarette smoke: a matter of exposure. Med. Hypotheses., **26**, 9-10.

Rotoli, B.M., Bussolati, O., Bianchi, M.G., Barilli, A., Balasubramanian, C., Bellucci, S. and Bergamaschi, E. (2008). Non-functionalized multi-walled carbon nanotubes alter the paracellular permeability of human airway epithelial cells. Toxicol. Lett., **178**, 95-102.

Simet, S.M., Sisson, J.H., Pavlik, J.A., Devasure, J.M., Boyer, C., Liu, X., Kawasaki, S., Sharp, J.G., Rennard, S.I. and Wyatt, T.A. (2010): Long-term cigarette smoke exposure in a mouse model of ciliated epithelial cell function. Am. J. Respir. Cell. Mol. Biol., **43**, 635-640.

Woodworth, C.D., Mossman, B.T. and Craighead, J.E. (1983): Squamous metaplasia of the respiratory tract. Possible pathogenic role in asbestos-associated bronchogenic carcinoma. Laboratory investigation; a journal of technical methods and pathology, **48**, 578-584.

Xu, J., Futakuchi, M., Alexander, D.B., Fukamachi, K., Numano, T., Suzui, M., Shimizu, H., Omori, T., Kanno, J., Hirose, A. and Tsuda, H. (2014): Nanosized zinc oxide particles do not promote DHPN-induced lung carcinogenesis but cause reversible epithelial hyperplasia of terminal bronchioles. Arch. Toxicol., **88**, 65-75.

Xu, J., Futakuchi, M., Shimizu, H., Alexander, D.B., Yanagihara, K., Fukamachi, K., Suzui, M., Kanno, J., Hirose, A., Ogata, A., Sakamoto, Y., Nakae, D., Omori, T. and Tsuda, H. (2012): Multi-walled carbon nanotubes translocate into the pleural cavity and induce visceral mesothelial proliferation in rats. Cancer Sci., **103**, 2045-2050.